TM-70-1011-5

TECHNICAL MEMORANDUM

ATMOSPHERIC X-RAY FLUORESCENCE

Bellcomm

NASA CR OR TMX OR AD NUMBER CATEGORY

BELLCOMM, INC.
955 L'ENFANT PLAZA NORTH, S.W., WASHINGTON, D.C. 20024

COVER SHEET FOR TECHNICAL MEMORANDUM

TITLE– Atmospheric X-ray Fluorescence

TM–70-1011-5

DATE–July 7, 1970

FILING CASE NO(S)– 103-7

AUTHOR(S)– F. F. Tomblin

FILING SUBJECT(S) (ASSIGNED BY AUTHOR(S))– X-ray Astronomy

ABSTRACT

Solar stimulated fluorescence by photoelectric ionization in the earth's upper atmosphere generates fluxes of up to 9×10^4 photons/cm^2 sec sr at 110 km for nitrogen K-α emission. The corresponding maximum flux for oxygen is 1×10^4 photons/cm^2 sec sr at approximately the same altitude. This flux may place a significant limitation on low energy (.1-1 keV) X-ray astronomy experiments which are performed during the daytime at altitudes below 300 km. Resonant K-α scattering is found not to contribute significantly to the photoelectric K-α generation.

SEE REVERSE SIDE FOR DISTRIBUTION LIST

DISTRIBUTION

COMPLETE MEMORANDUM TO

CORRESPONDENCE FILES:

OFFICIAL FILE COPY
plus one white copy for each additional case referenced

TECHNICAL LIBRARY (4)

NASA Headquarters

W. O. Armstrong/MTX
P. E. Culbertson/MT
M Dubin/SG
D. L. Forsythe/MLA
H. Glaser/SG
E. W. Hall/MTG
H. Hall/MTX
T. A. Keegan/MA-2
R. L. Lohman/MF
D. R. Lord/MF
J. L. Mitchell/SG
L. Roberts/OART-M (2)
N. G. Roman/SG
A. D. Schnyer/MTV
H. J. Smith/SS
M. F. Waugh/MTP
J. W. Wild/MTE

Goddard Space Flight Center

G. E. Fichtel/611.2

Marshall Space Flight Center

J. A. Downey/PD-MP-DIR
R. E. Lake/S&E-R-F
E. Stuhlinger/AD-S

Manned Spacecraft Center

S. C. Freden/TG
O. K. Garriott/CB
K. G. Henize/CB

COMPLETE MEMORANDUM TO

Bellcomm, Inc.

G. M. Anderson
D. O. Baechler
A. P. Boysen, Jr.
J. O. Cappellari, Jr
C. L. Davis
D. A. DeGraaf
J. P. Downs
D. R. Hagner
E. E. Hillyard
N. W. Hinners
D. B. James
H. S. London
P. F. Long
D. Macchia
E. D. Marion
K. E. Martersteck
W. I. McLaughlin
J. Z. Menard
J. W. Nervik
G. T. Orrok
I. M. Ross
S. A. Schelke
J. W. Timko
A. R. Vernon
J. E. Volonte
R. L. Wagner
M. P. Wilson
D. B. Wood
All Members Depts. 1011, 1012 and 1013
Department 1024 File
Central File
Library

BELLCOMM, INC.
955 L'ENFANT PLAZA NORTH, S.W. WASHINGTON, D. C. 20024

SUBJECT: Atmospheric X-ray Fluorescence
Case 103-7

DATE: July 7, 1970

FROM: F. F. Tomblin

TM-70-1011-5

TECHNICAL MEMORANDUM

1.0 INTRODUCTION

The primary constituents of the earth's upper atmosphere, oxygen and nitrogen, are subject to ionizing solar radiation with energy sufficient to remove the K-shell electrons from these atoms. Therefore, characteristic fluorescence is to be expected. We shall compute the daytime fluorescence intensity variation as a function of altitude and direction for various positions of the sun.

The fluorescent radiation is monochromatic because the dominant radiative mechanism for reorganization of the atomic electrons results in an L-shell electron filling the vacant K-shell. Such transitions result in K-α radiation with energy equal to the difference in binding energy of the K and L shells. Similar transitions from the M to the K shell are classified K-β transitions. Since the energy levels of the L and M shells are quite closely spaced compared with the K-L energy difference, the energies of the K-α and K-β transitions are nearly equal.

The atmospheric X-ray fluorescence calculation requires a knowledge of the solar X-ray flux spectrum at energies greater than the ionization potential for the atom in question (.4 keV for nitrogen). The atomic atmospheric density and the photoionization cross section are also required. The K-shell photoionization cross section is a measure of the probability that an X-ray of a given wavelength can ionize an atom by removal of the K-shell electron.

Since these calculations involve elements with a low atomic number, not all K-shell ionizations result in the subsequent emission of a K-α photon. In fact radiationless transitions result in most cases. Energetic Auger electrons remove the excess energy. The fluorescence yield, ω_k, is defined as the probability that a radiative transition will occur subsequent to K-shell ionization. For the light elements considered here this probability is on the order of a fraction of a percent. ω_k enters the calculations for the fluorescence of the atmosphere as a multiplicative constant for each atomic species. Auger electron emission and radiative decay are described pictorially in Figure 1.

Until very recently, fluorescence yields for atoms and ions with $Z < 15$ were very poorly known. Experimental results often disagreed by orders of magnitude. McGuire (1960 and 1970) has computed the fluorescence yields of these elements using atomic potentials, $-rV(r)$, obtained by Herman and Skillman (1963). The potential is approximated by a series of straight line segments resulting in an exactly solvable wavefunction. McGuire's (1970) results are used here and should be accurate to $\pm 25\%$.

For future reference we list in Table 1 the K-shell ionization energy, E(1s); the K-α transition energy, E(K-α), (both in ev) as given in Bearden (1967); and ω_k, the fluorescence yield, as computed by McGuire (1970).

Table 1

ATOMIC X-RAY EMISSION PROPERTIES

	E(1s)		E(K-α)		
Atom	ev	Å	ev	Å	ω_k
Nitrogen	400	30.99	392	31.60	6.0×10^{-3}
Oxygen	532	23.32	525	23.62	9.4×10^{-3}

The K-α energies listed are those of singly ionized atoms. One electron in the 2p state is removed in the stable state of such ions. In the case of photoionization, electrons falling from the 2p state to the 1s state give rise to the K-shell fluorescence. Variations on the order of 1% are to be anticipated for the K-α radiation for singly ionized atoms or atoms in various molecular situations.

When solar radiation falls in the naturally broadened line envelope which corresponds to the K-α transition, the atom may be excited with high probability. Again, the dominant mode of de-excitation is by autoionization, and it will be shown that this scattered radiation is probably not of sufficient intensity to be observable.

Our results on atmospheric fluorescence should be of considerable interest to experimenters developing plans for low earth orbit X-ray astronomy missions covering the 20-40 Å region. Daytime studies of stellar X-ray sources using non-dispersive detectors may be difficult to perform due to this fluorescence.

2.0 THE GENERATION OF K-α EMISSION

In this calculation it is assumed that the solar XUV emission photoionizes the atomic species. The subsequent fluorescence is then observed corresponding to the 1s-2p transition. It is important to note that this is not the same mechanism responsible for the hydrogen Lyman-α geocorona. In the case of hydrogen Lyman-α, the sun emits strongly at 1216Å. This radiation is resonantly scattered by atomic hydrogen. The autoionization process is, of course, not applicable for one electron atoms. Resonant scattering will be shown to contribute a negligible amount of K-α emission from neutral atoms.

The unattenuated solar X-ray flux passing through an element of surface normal to the sun is given by:

$$f_s(\lambda) = \frac{dN(\lambda)}{d\ \lambda} \text{ photons/cm}^2\text{sec Å}$$

If the atmospheric density of the atomic species i is $\rho_i(h)$ at altitude h, and the cross section for the K-shell photoelectric effect is $\sigma_i(\lambda)$, the total number of fluorescent photons generated per volume element dV is

$$\frac{dN_i(h)}{dV} = \int_0^{\lambda_c} d\lambda \; f_s(\lambda) \; \sigma_{k_i}(\lambda)\rho_i(h) \; \omega_{k_i} \qquad (1)$$

where λ_c is the critical wavelength corresponding to the K-shell ionization edge.

The K-shell photoelectric cross section has been measured (Allen, 1959) and computed theoretically (McGuire, 1967). The results are in excellent agreement. The theoretical curves are shown in Figure 2. The 2s and 2p (L-shell) cross sections are considerably smaller, but they do contribute to the total absorption. These values are shown separately in Figure 2.

An accurate representation of the absolute solar flux from 10 to 30 Å is not available. Only approximate representation of the solar spectral shape is required at most wavelengths because the solar flux is weighted by the photoelectric cross section as indicated by equation (1). However, accurate knowledge of the absolute flux level near the absorption edge is needed for reliable results. We have taken the results of Mandelstam (1965) using $T_e = 3\times10^6$ °K as the primary source of quiet solar spectral information for wavelengths less than 25 Å. Adjustments were necessary to correct the oxygen and iron line emissions computed by Mandelstam between 13 and 22 Å for the line intensity observed in the corona. The absolute spectral data of Evans et al (1968) was used for this correction. A check on the total emission from 8 - 20 Å can be made using the data of Kreplin et al (1969) taken of the quiet sun during the intermediate period of the solar cycle in 1967. No experimental data is available in the 25 - 30 Å region. Beigman et al (1969) indicate in their theoretical results that there are no significant emission lines in this region except at 28.8 Å. They indicate a value of $\sim 10^{-3}$ ergs/cm^2 sec Å for this line. A continuum level of 6×10^{-4} ergs/cm^2 sec Å is used for the 25 - 32 Å region. This value is taken from the calculations of Mandelstam (1965) at 20 Å and is consistent with the spectral observations taken by Manson (1967) in the 30 - 31 Å interval. There should be no large changes in the continuum level over the 25 - 32 Å region. The composite spectrum is shown in Figure 3.

To complete the necessary experimental data, the atmospheric density profile of the O, O_2 and N_2 composition is necessary. For the purpose of the calculation we assume an exospheric temperature of 1000°K. This temperature is typical of the period intermediate between solar maximum and minimum. The spring/fall data of the US Standard Atmosphere Supplements, (1966) given in Figure 4 is used in calculations.

3.0 COMPUTATION TECHNIQUES

a. General Formalism

There are a number of cases which may be considered for which the geometry is not unnecessarily complex. Each depends on the zenith angle of the sun, look direction, and altitude. These variables are defined as shown in Figure 5.

Note that θ' is the angle from the local normal to the solar direction and θ is the angle the look direction makes with the local normal. We will consider only situations where the line of sight lies in the plane formed by the local vertical direction and the solar direction.

There are two essential modifications to equation (1) required to complete this calculation. First, atmospheric absorption of solar radiation above the point h*, where ionization occurs, must be considered. This includes the entire solar flux with energy in excess of the ionization potential of the atom.

This absorption is by the photoelectric effect; thus the total cross sections given in Figure 2 may be used. The fraction of solar radiation passing through the atmosphere is

$$F(\lambda, h^*, \theta') = \mathrm{EXP}\left(-\sum_i \int_{h^*}^{\infty} \sigma_{T_i}(\lambda)\rho_i(h')dh'\sec\theta'\right). \quad (2)$$

$\sigma_{T_i}(\lambda)$ is the absorption cross section as a function of wavelength for each species; $\sec\theta'$ is the correction to the absorption path for a non-zero solar zenith angle.

The second feature for which a correction must be made is atmospheric absorption of the K-α radiation from the point of generation h* to the point of observation h along the line of sight. This has a form similar to equation (2) except that the absorption cross section σ_{T_i} is evaluated at the K-α wavelength only.

The attenuation of the X-ray strength at h is

$$G_i(\lambda_\ell,h,h^*,\theta) = \mathrm{EXP}\left(-\sum\int_h^{h^*}\sigma_{T_i}(\lambda_\ell)\rho_i(h')\,dh'\sec\theta\right) \quad (3)$$

The generation of X-rays along the line of sight may occur from altitudes h and above.

Expression (1) may be modified by (2) and (3) to give the solar stimulated K-α X-ray fluorescence at altitude h from atomic species i:

$$N_i(h,\theta,\theta') = \frac{1}{4\pi}\int_0^{\lambda c}\int_h^{\infty}\omega_{k_i}\sigma_{k_i}(\lambda_\ell)f_s(\lambda)\rho_i(h^*)\sec\theta\, F_i(\lambda,h^*,\theta')\, G_i(\lambda_\ell,h,h^*,\theta)\,d\lambda dh^* \quad (4)$$

Equation (4) should not be considered valid for θ and θ' much larger than 60° as the curvature of the earth has not been considered.

b. <u>Fluorescence Albedo (θ=180°)</u>

The upward-directed fluorescent radiation (albedo) may be calculated by reversing the order of integration of equations (3) and (4). Looking at the nadir (θ=180°) the upward-directed flux becomes

$$N_i(h,\theta,\theta') = \frac{1}{4\pi}\int_0^{\lambda c}\int_0^{h}\omega_{k_i}\sigma_{ki}\rho_i(h^*)f_s(\lambda)\; F_i(\lambda,h^*,\theta')G_i(\lambda_\ell,h,h^*\theta)\,d\lambda dh^*$$

c. <u>Fluorescence at θ=90°</u>

One of the brightest regions of fluorescent X-rays is in the plane normal to the local vertical. Here the X-ray generation path, h to h*, is quite long and the flux will reach its maximum at a higher altitude than when viewing at smaller zenith angles. The path length is corrected to consider the curvature of the earth and atmosphere. This is done by replacing dh* by $\sqrt{\frac{R_e}{2(h^*-h)}}\,dh^*$ and making appropriate modifications to F_i and G_i.

Modifying equation (4) to include the effects of the earth's curvature

$$N_i(h,90°,\theta') = \frac{1}{4\pi}\int_0^{\lambda c}\int_h^{\infty}\omega_{k_i}\sigma_{k_i}(\lambda)\rho_i(h^*)f_s(\lambda)\sqrt{\frac{R_e}{2(h^*-h)}}\,F_i'(\lambda,h,h^*,\theta')$$

$$G_i'(\lambda_\ell,h,h^*)\;dh^*d\lambda$$

where

$$G_i'(\lambda_\ell,h,h^*) = \mathrm{EXP}\left(-\sum_i\int_h^{h^*}\sigma_{T_i}(\lambda_\ell)\rho_i(h')\sqrt{\frac{R_e}{2(h'-h)}}\,dh'\right)$$

$$F_i'(\lambda,h,h^*,\theta') = \mathrm{EXP}\left[-\sum_i\int_{h^*}^{\infty}\sigma_{T_i}(\lambda)\rho_i(h')\quad\sec\left(\theta' \pm \tan^{-1}\sqrt{\frac{2(h'-h)}{R_e}}\right)dh'\right]$$

R_e = radius of the earth 100 km above the atmosphere (6500 km); the +(-) sign is used in F_i when θ and θ' have different (the same) sign. (See Figure 5.)

4.0 RESULTS

The calculations for representative cases of atomsphere fluorescence are given in Figures 6 and 7 for oxygen and nitrogen. Figure 6 shows the detailed nature of the K-α emission below 200 km where the differences in orientation are most striking. Figure 7 indicates the magnitude of the oxygen and nitrogen line intensities at higher altitudes.

Several important features of atmospheric fluorescence are apparent from these figures. Below 150 km the intensity of the nitrogen line exceeds that due to oxygen. This is due to the larger photoelectric cross section for nitrogen in the 25 - 31 Å region and the larger nitrogen abundance in the atmosphere. The photoabsorption by nitrogen attenuates the radiation in the wavelength region near the K-α line of oxygen at altitudes below 120 km. Atmospheric absorption of the nitrogen K-α emission is only appreciable at altitudes below 110 km. For this reason, the maximum for the nitrogen emission is observed at a slightly lower altitude than the maximum for oxygen.

Above 150 km atmospheric absorption becomes unimportant and the K-α emission becomes proportional to the partial pressure of the constituent gasses. The N_2 density falls off with an e-folding height of $\sim$35 km at altitudes above 200 km; the oxygen density falls off more slowly with an e-folding height of $\sim$65 km. Thus, above 300 km the oxygen K-α emission dominates that due to nitrogen.

Variations in the elevation angle of the sun affect the fluorescence only at low altitudes near the intensity maximum. The fluorescence at $\theta'=60°$ appears to be reduced over that observed for $\theta'=0$ along the same line of sight. As expected, viewing near the horizon ($\theta=90°$) gives the most intense radiation of the various cases considered for both O and N_2.

The albedo fluorescence is relatively unchanged at altitudes above 130 km. The atmospheric fluorescence generated above this altitude is negligible compared to that generated in the 100 - 125 km layer.

Calculations have been performed concerning the contribution of resonantly scattered X-rays. The results are given in detailed form in the appendix. It is shown that the resonantly scattered component contributes less than 1% of the flux which can be attributed to the fluorescent radiation process.

Grader et al (1968) have observed daytime atmospheric fluorescence at energies above 400 eV. This experiment was performed from a rocket at altitudes up to 190 km. The field of view was approximately ±30° from the 90° zenith orientation. The total intensity of the K-α line of nitrogen may not have been observed in this experiment; however, count rates of $5000/cm^2 sec\ sr$ were observed. This value is slightly smaller than the maximum rate computed here for oxygen, but much less than the computed nitrogen rate. The wide field of view used for this experiment makes a detailed altitude-count rate correlation difficult. However, it is certainly a verification of the existence of the daytime fluorescence. It should be pointed out that the mechanism ascribed to this effect by Grader et al is the excitation of terrestrial nitrogen and oxygen by the N VII and O VII solar lines. While these lines do make a significant contribution to the observed fluorescence level, the entire solar continuum and line emission above 12 Å must be considered to account for the observed flux.

5.0 SIGNIFICANCE FOR GALACTIC X-RAY ASTRONOMY

Recently interest in celestial observations over the wavelength region from 44 - 60 Å has increased. This is primarily due to the observation of unexpectedly strong emission from the region near the galactic pole (Fritz et al, 1968). Yet few measurements of X-ray sources have been made between 44 and 20 Å due to the poor energy resolution of detectors currently in use for this wavelength region.

The X-ray background flux has been measured extensively below 10 Å and a few experiments have been conducted above 44 Å by Henry et al (1968) and Bowyer et al (1968). By interpolation of this data one can conclude that the isotropic flux in the 10 Å interval about 23 Å is $\sim$10 photons/cm^{2}sec sr and slightly higher at 31 Å. (10 Å is about the best energy resolution which can be obtained from a proportional counter at 23 Å). Thus at altitudes below 300 km, the fluorescence of K-α emission from oxygen alone will exceed the galactic background level for all look directions when proportional counters are used. Moreover, the atmospheric fluorescence rate is directly coupled to solar emission. A moderate level of solar flux was assumed for these calculations. Yet flares may cause increases of 100 - 500% in the 15 - 30 Å emission over a period of 10-30 minutes, increasing K-α fluorescence by an equivalent amount during such solar activity.

The major uncertainty in these results is caused by inadequate knowledge of the absolute solar flux in the 15 - 30 Å region. The integrated effect of this error in these calculations is probably 100%. Uncertainties in the atmospheric density profile are probably somewhat smaller than this and subject to more systematic variations with solar cycle.

Verification of the individual K-α intensities computed here may be difficult because of the low energy resolution currently available from non-dispersive detectors. However, solid state lithium drifted silicon detectors which will soon be in use should have an energy resolution of ∿100 eV in the region of interest. This should be adequate to separate the oxygen and nitrogen K-α lines. A well collimated array of such detectors flown on a rocket to an altitude of 200 km should obtain ample information on the altitude profile of this emission.

Fred Tomblin

1011-FFT-sh F. F. Tomblin

APPENDIX

Resonant Scattering

Resonant excitation concerns the absorption and reemission of radiation within the natural line width profile of the transition to be excited. The natural width due to the short lifetime of the excited state ($\tau=5\times10^{-13}$ sec) is $\sim$.1 eV (5×10^{-3} Å) full width half maximum. This is much greater than the 10^{-3} eV doppler broadening due to the thermal effects of the 1000°K effective ion temperature in the upper atmosphere.

The total cross section for resonant absorption may be written as

$$\sigma_i(E) = \sigma_{o_i} \frac{(\Gamma_i/2)^2}{(E_{o_i}-E)^2 + (\Gamma_i/2)^2}$$

where Γ_i is the line width and E_{o_i} is the resonant energy,

$$\sigma_{o_i} = \frac{e^2 h f_{12_i}}{\pi m c \Gamma_i} ,$$

$\frac{e^2}{mc^2} = 2.82\ 10^{-13}$ cm (classical radius of electron), and

f_{12_i} is the oscillator strength.

VALUES OF PARAMETERS

	Γ_i^* (ev)	f_{12_i}*	σ_{o_i} ($\times10^{-17}$ cm^2)
Oxygen	.145	.17	1.2
Nitrogen	.095	.14	1.3

*Computed from results listed by McGuire (1969).

The resonance interaction has two important aspects: 1) resonant absorption of fluorescent line radiation 2) scattering of solar continuum radiation. The first of these concerns the absorption of the O^+ or N_2^+ K-α radiation computed in the previous section by similar species present in the upper atmosphere.

The maximum density of O^+ is 7×10^5/cc at 300 km (Anderson and Francis, 1964) and falls off rapidly at altitudes below 150 km and above 500 km. The mean free-path for resonant absorption of the O^+ K-α line is therefore 12×10^6 km at 300 km: much too large to be significant. The N_2^+ density never exceeds 10^4/cc (Ghosh, 1968) and is likewise insignificant.

The scattering of solar continuum radiation at the K-α energy is possible and the calculation of the scattered intensity is straightforward. Here we are concerned with the direct excitation of the O and N_2 K-α line. The scattered radiation will be subject to loss by resonant absorption of O and N_2. Most of this absorbed radiation is not reradiated, but lost to autoionization.

The flux of resonantly scattered solar X-rays is now computed to establish its importance relative to the fluorescence levels previously computed. To simplify the notation we will denote the line shape by

$$L_i(E,\Gamma) = \frac{(\Gamma_i/2)^2}{(E-E_{O_i})^2 + (\Gamma_i/2)^2}$$

Thus the line radiation reaching an altitude h is

$$N_i(h) = \frac{1}{4\pi}\int_0^\infty f_s \int_h^\infty \rho_i(h')\sigma_{o_i} L_i(E,\Gamma)\,dE \int_0^\infty \left\{L_i(E',\Gamma)\frac{dE'}{(\Gamma/2)}\ 1/\pi\ \omega_{k_i}\right\}$$
$$\times \left\{\mathrm{EXP} - \int_{h'}^\infty \rho_i(h'')\sigma_{o_i}\ L_i(E,\Gamma)\,dh''\right\}$$
$$\times \left\{\mathrm{EXP} - \int_h^{h'} \rho_i(h'')\sigma_{o_i}\ L_i(E',\Gamma)\,dh''\right\} dh'\,dE'\,dE \qquad (5)$$

f_s, the solar flux at the K-α line (with units of photons/cm^2 sec eV), is assumed flat over the line width. The first bracketed term is the line shape, the second is the probability of absorption prior to scattering and the third is the probability of absorption following scattering.

For the case where absorption is small, $N_i(h)$ may be expressed analytically as

$$N_i(h) = \frac{1}{16}\, f_s\ \omega_{k_i}\ \Gamma_i\ \sigma_{oi} \int_h^\infty \rho_i(h')\,dh' \qquad (6)$$

Using (5) and (6) at the appropriate altitudes with $f_s = 3\times10^4$ photons/cm^2 sec eV at the oxygen K-α line results in a maximum resonant scattering intensity at 130 km of 1.5 photons/cm^2 sec sr. At the nitrogen K-α line $f_s = 7\times10^4$ photons/cm^2 sec eV, giving a maximum intensity for the scattered K-α flux of 2.5 photons/cm^2 sec sr at 130 km. At altitudes below 130 km considerable self absorption occurs. These resonantly scattered flux levels are less than 1% of that computed for the K-α fluorescence emission.

Other resonantly scattered radiation, such as K-β may contribute some additional flux; however, the total contribution from such sources will be insignificant when compared with the natural variations in the fluorescent radiation. These variations are caused by solar flares and long term oscillations in the atmospheric densities associated with periodicity of the solar cycle.

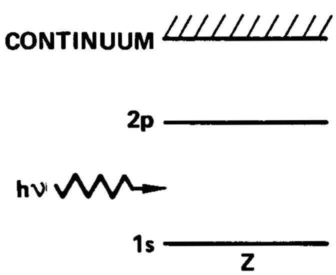

a) SIMPLIFIED ENERGY LEVEL DIAGRAM BEFORE PHOTO-IONIZATION

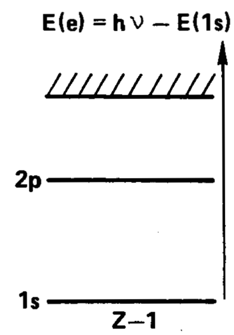

b) PHOTOIONIZATION REMOVING THE K SHELL ELECTRON. EXCESS ENERGY = E(1s)

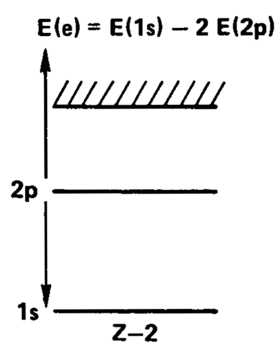

c) AUTOIONIZATION REFILLS THE 1s LEVEL AND EJECTS AN ELECTRON TO REMOVE EXCESS ENERGY

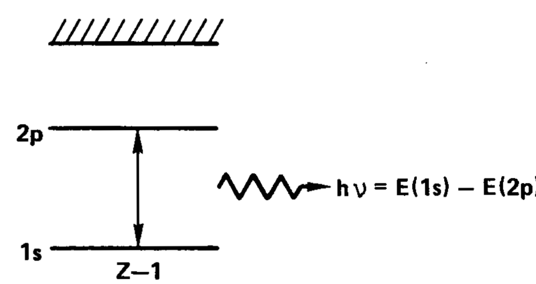

d) RADIATIVE DECAY (AN ALTERNATIVE TO PROCESS c)) TO REMOVE EXCESS ENERGY.

FIGURE 1. THE AUTOIONIZATION PROCESS AND RADIATIVE DECAY FOLLOWING PHOTOIONIZATION.

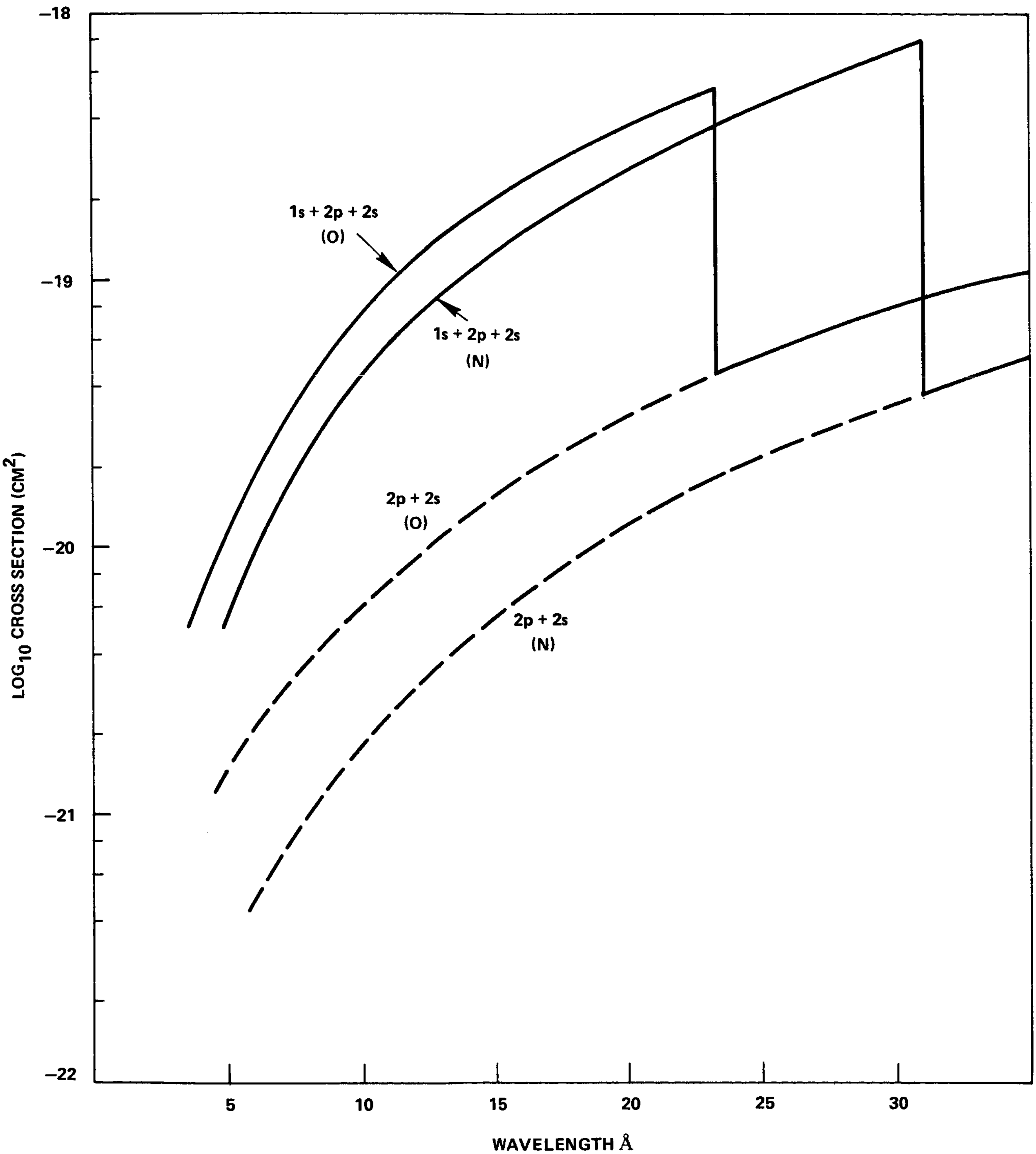

FIGURE 2. PHOTOELECTRIC CROSS SECTION VS WAVELENGTH FOR THE K AND L SHELLS OF OXYGEN AND NITROGEN.

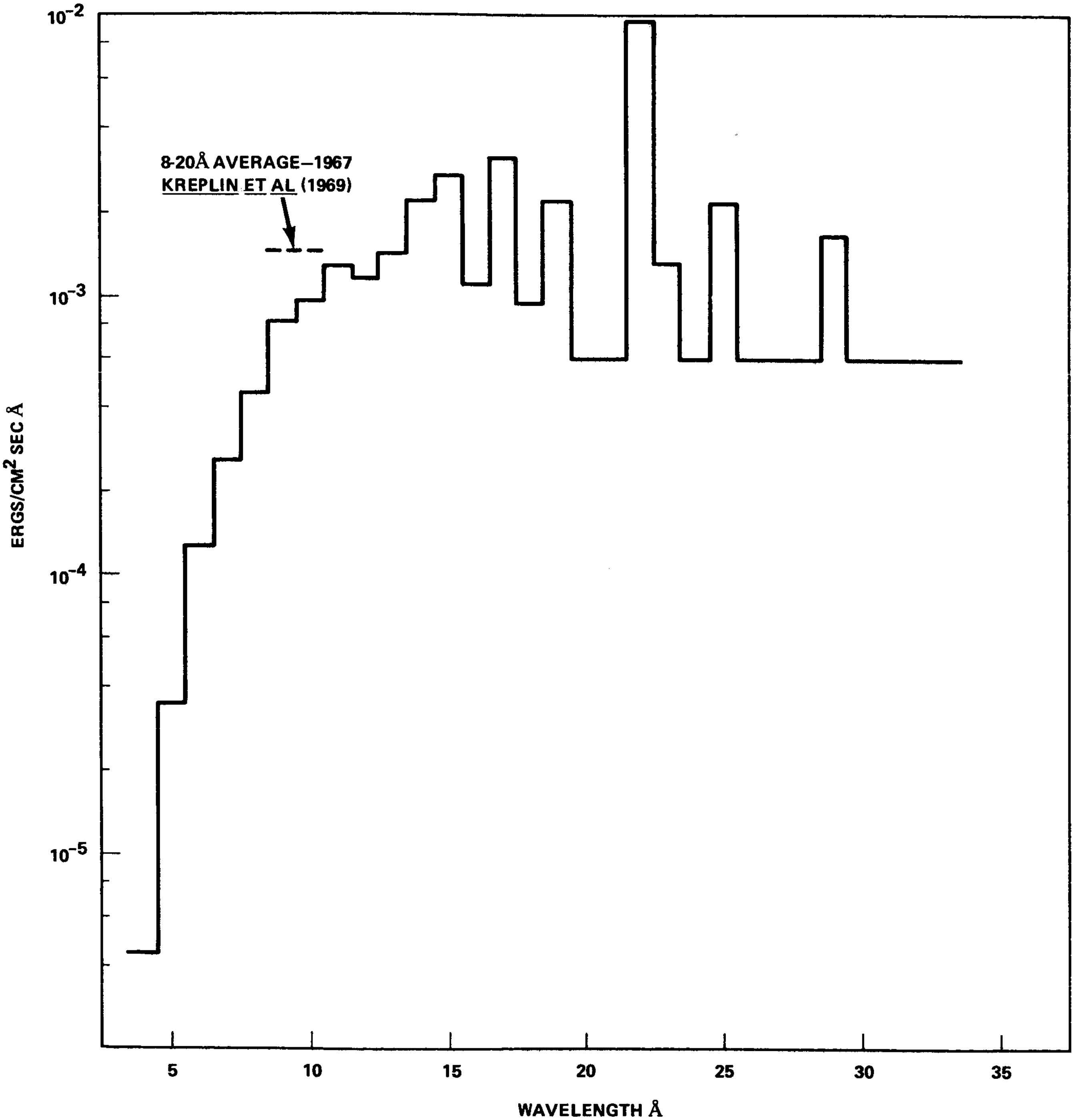

FIGURE 3. COMPOSITE SOLAR SPECTRUM FROM EXPERIMENTAL AND THEORETICAL DATA.

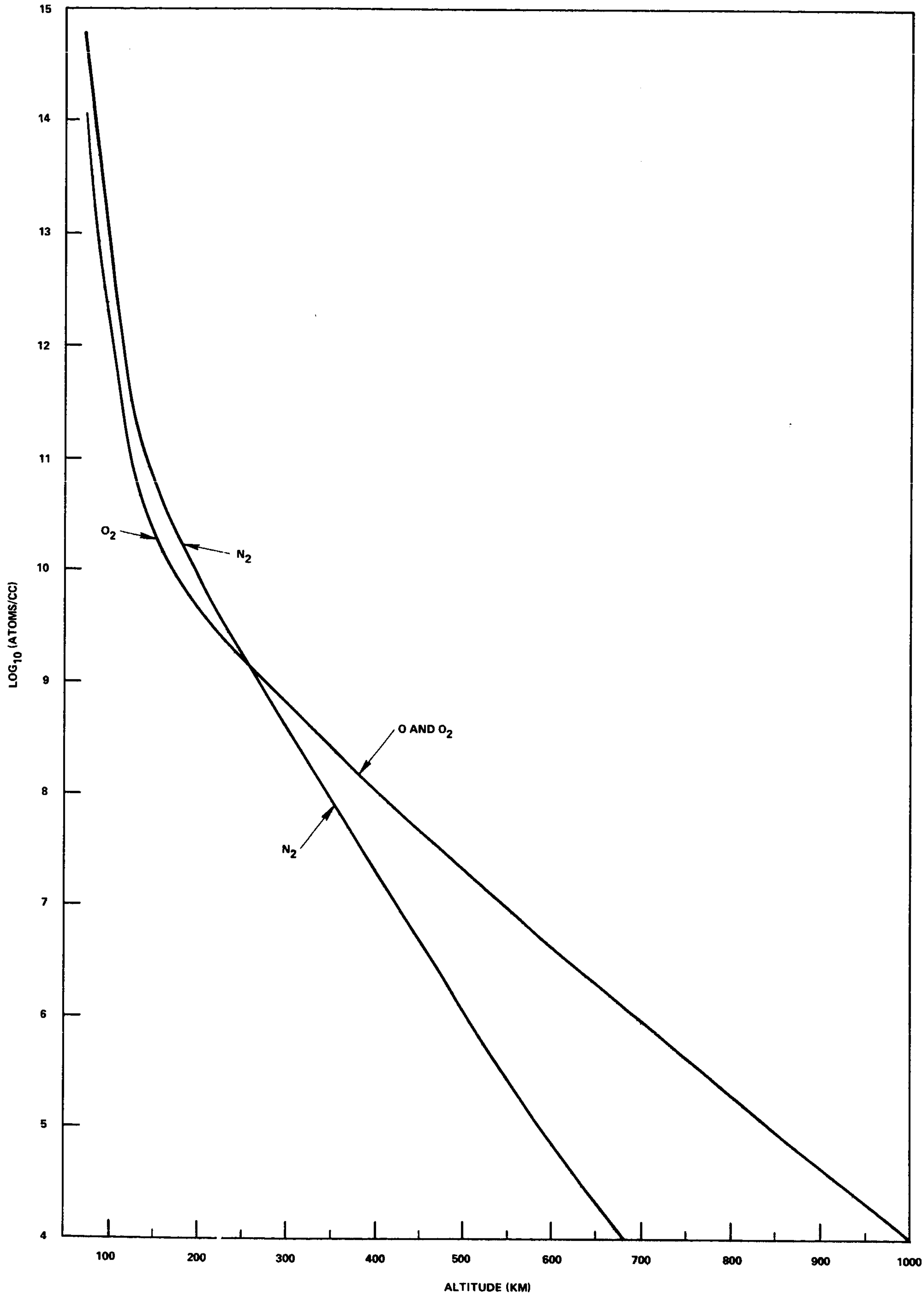

FIGURE 4. SPRING/FALL MODEL ATMOSPHERE WITH 1000°K EXOSPHERIC TEMPERATURE, U.S. STANDARD ATMOSPHERE SUPPLEMENTS (1966).

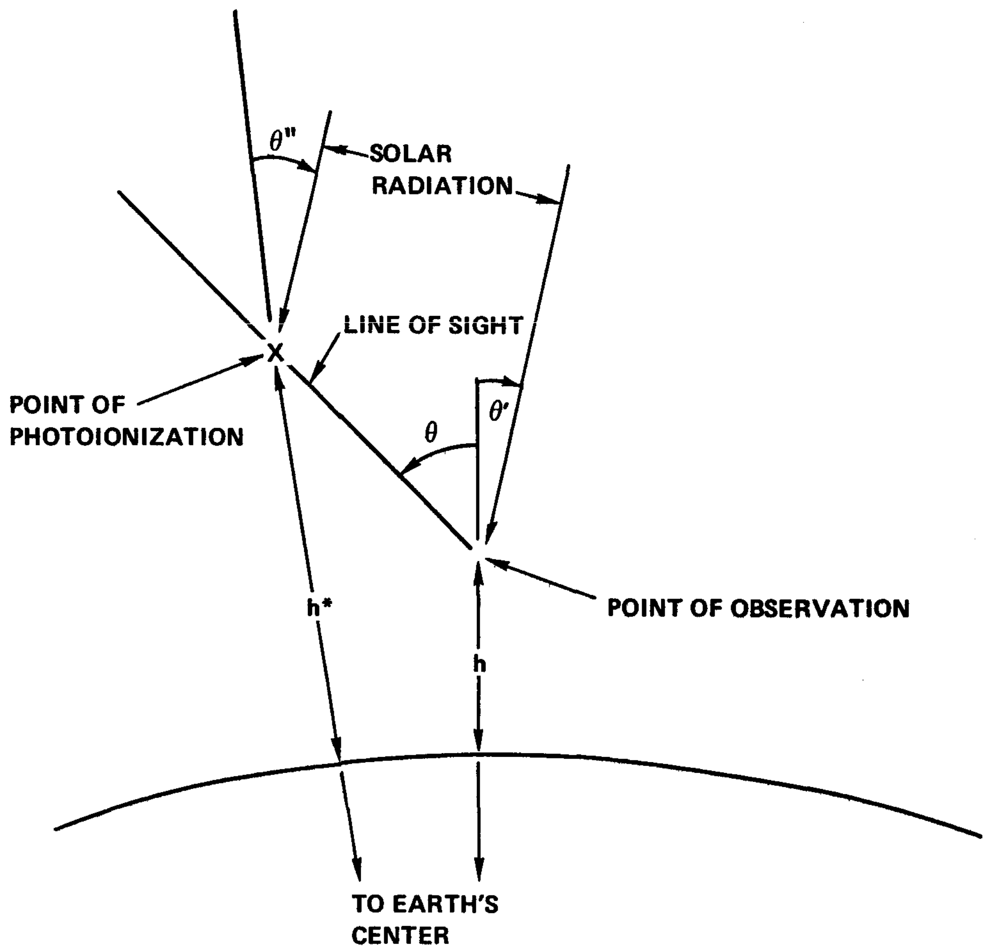

FIGURE 5. THE GEOMETRIC CONFIGURATION OF THE VARIOUS FACTORS FOR CALCULATION OF K-α FLUORESCENCE. THE CONVENTION ADOPTED FOR ANGLES IS THAT θ IS NEGATIVE AND θ' IS POSITIVE AS SHOWN IN THE FIGURE.

θ'' IS ASSUMED EQUAL TO θ' FOR $\theta < 60°$. WHEN $\theta = 90°$ θ'' IS CORRECTED AS INDICATED IN EXPRESSION FOR F'.

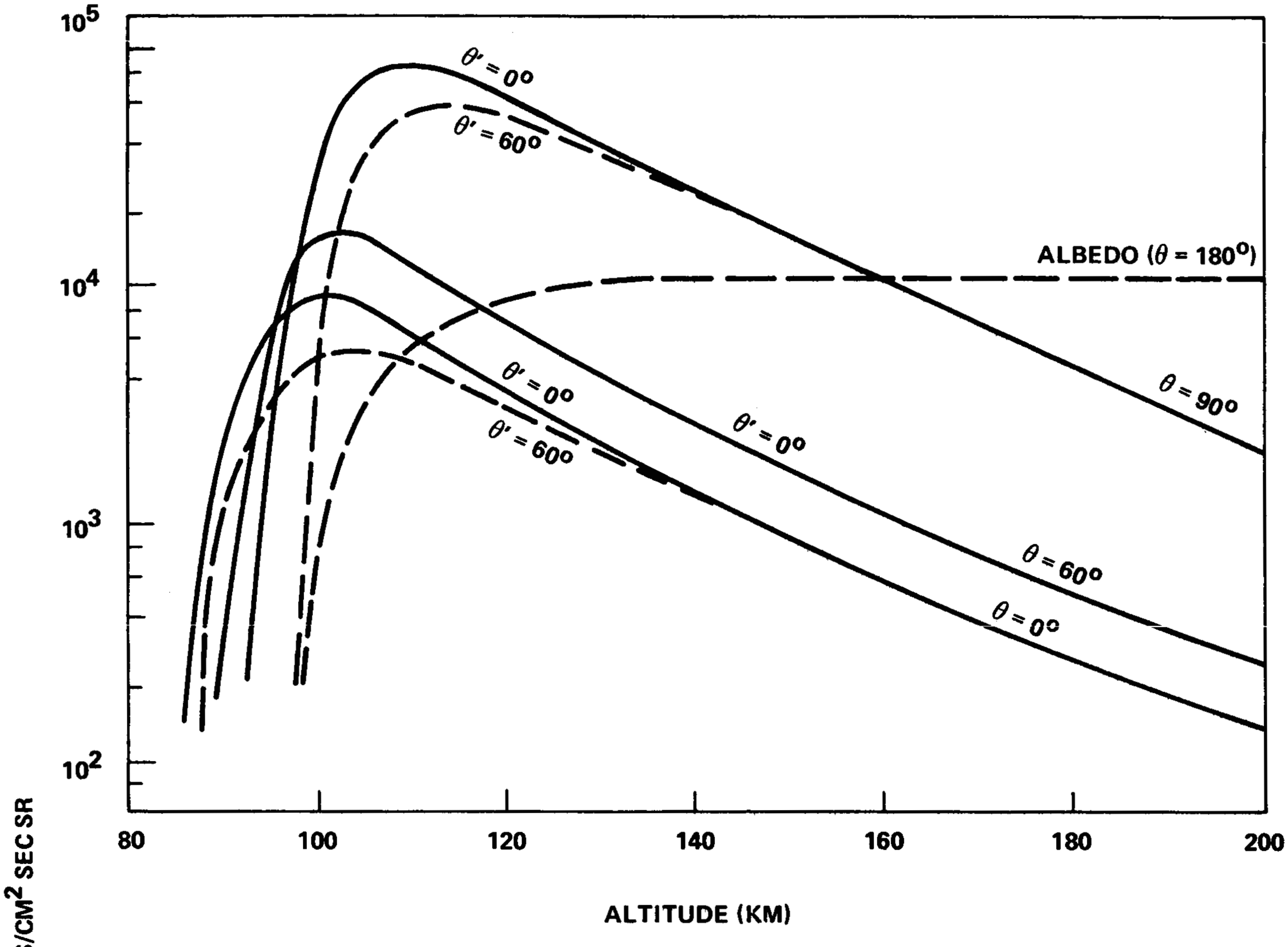

FIGURE 6A. NITROGEN K-α EMISSION AS A FUNCTION OF OBSERVING ALTITUDE (h)

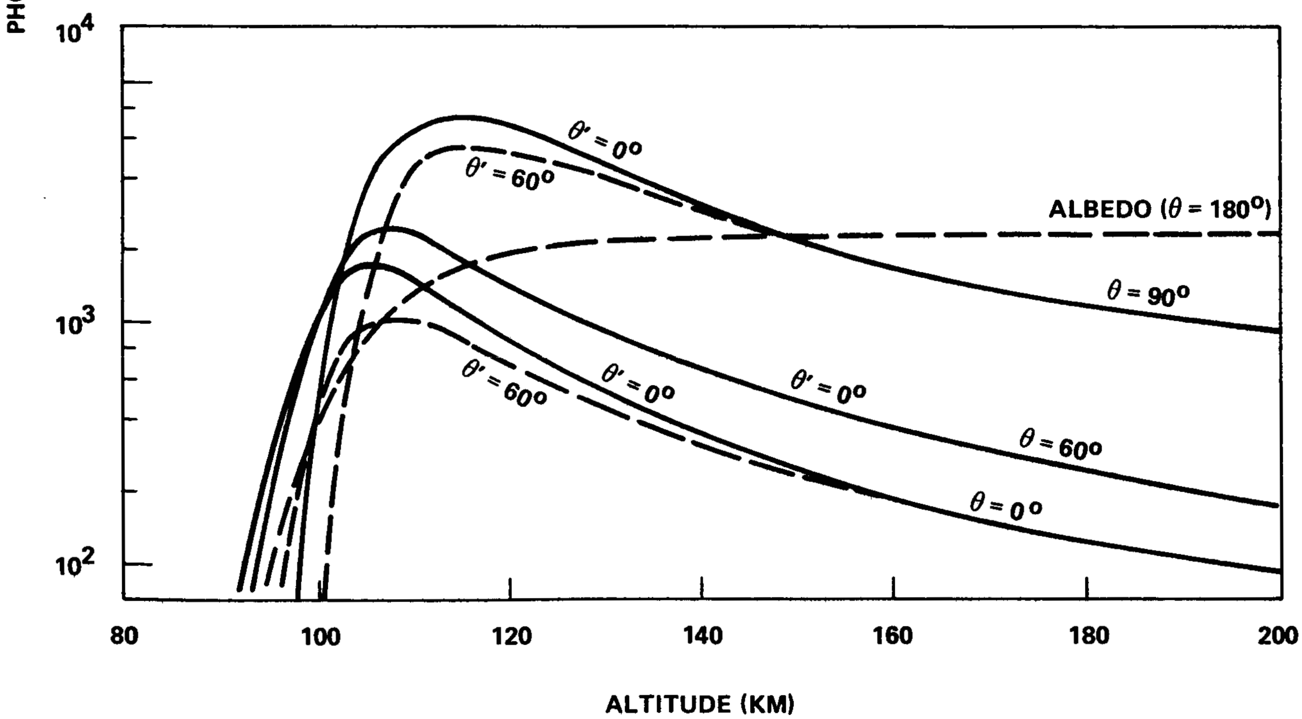

FIGURE 6B. OXYGEN K-α EMISSION AS A FUNCTION OF OBSERVING ALTITUDE (h)

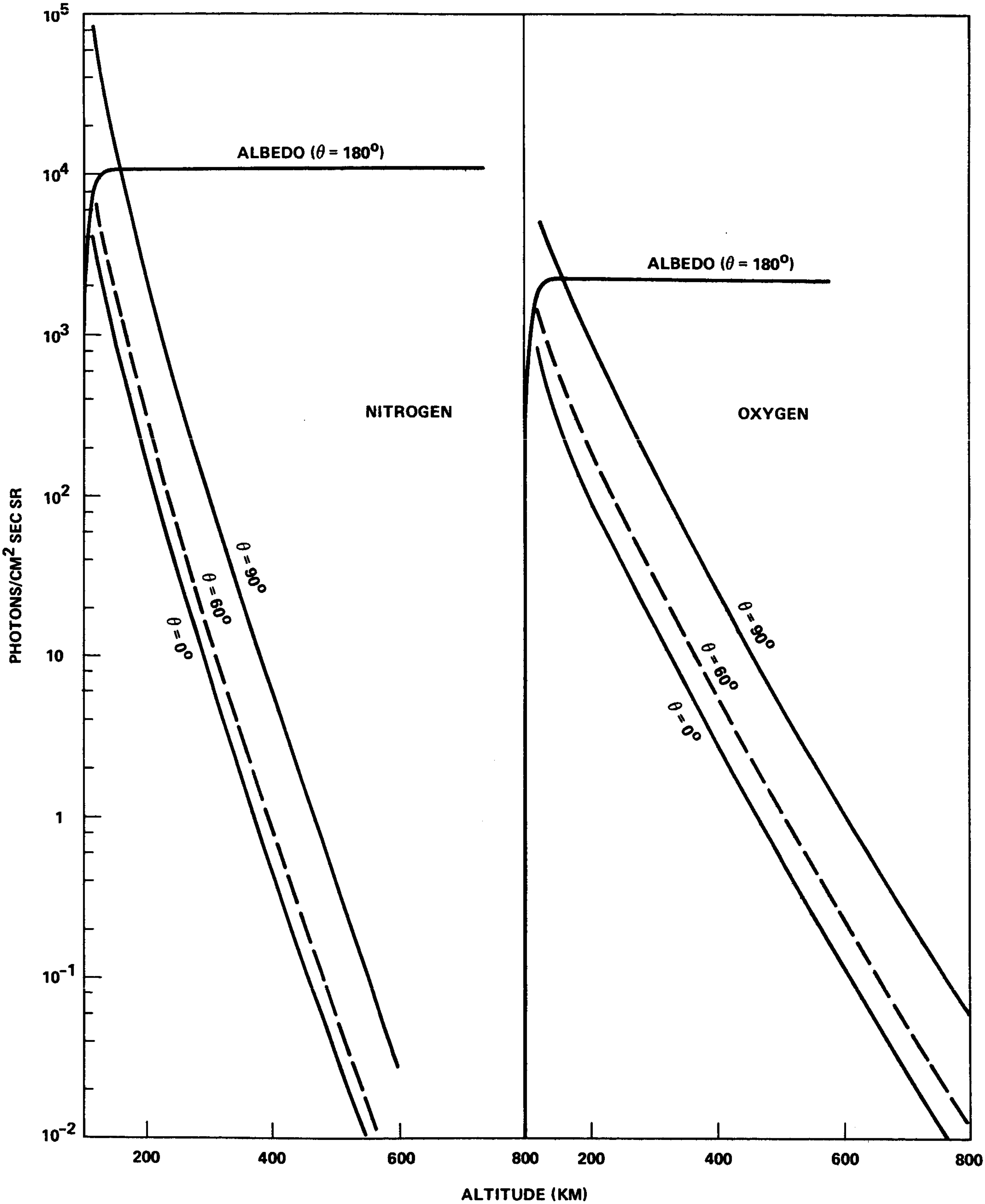

FIGURE 7. K-α FLUORESCENCE FOR OXYGEN AND NITROGEN IN VARIOUS DIRECTIONS AS A FUNCTION OF OBSERVATION ALTITUDE FOR AN OVERHEAD SUN.

REFERENCES

Allen, S. M. J., Handbook of Chemistry and Physics, 40th ed. 1959 p.2660 Chemical Rubber Publishing Company, Cleveland, Ohio.

Anderson and Francis, Lockheed Missiles and Space Company, Report No. 6-74-64-19.

Bearden, J. A., Reviews of Modern Physics, 31, 1 (1967).

Beigman, I. L., L. A. Vainshtein, Kosmish. Issled. (in press).

Boyer, C. S., G. B. Field, J. E. Mack, Nature, 217, 32 (1968).

Evans, K. and K. A. Pounds, Ap.J., 152, 319 (1968).

Ghosh, S. N., J. Geophys. Res., 73, 309 (1968).

Grader, R. J., R. W. Hill, F. D. Seward, J. Geophys, Res., 73, 7149 (1968).

Henry, R. C., G. Fritz, J. F. Meekins, H. Friedman and E. T. Byram, Ap.J., 153, L11 (1968).

Herman, F., and S. Skillman, Atomic Structure Calculations, Prentice-Hall, Inc., Englewood Cliffs, N. J., (1963).

Kreplin, R. W., D. M. Horan, T. A. Chubb and H. Friedman, presented at the XI COSPAR Meeting, July (1968).

Mandelshtam, S. L., Annals d' Astrophysique, 28, 1 (1965).

Manson, J. E., Ap.J., 147, 703 (1967).

McGuire, E. J., Phys. Rev., 175, 20 (1968).

McGuire, E. J., Phys. Rev. 185, 1 (1969)

McGuire, E. J.. Phys, Rev., (1970) to be published.

U. S. Standard Atmosphere Supplements, 1966, U. S. Government Printing Office, Washington, D. C.